



Topographic and vegetation controls of the spatial distribution of snow depth in agro-forested environments by UAV-lidar

Vasana Dharmadasa^{1,2,3,5}, Christophe Kinnard^{1,2,3}, and Michel Baraër^{4,5}

¹Department of Environmental Sciences, University of Québec at Trois-Rivières, QC G8Z 4M3, Canada

5 ²Center for Northern Studies (CEN), Québec City, QC GV1 0A6, Canada

³Research Centre for Watershed-Aquatic Ecosystem Interactions (RIVE), University of Québec at Trois-Rivières, Trois-Rivières, QC G8Z 4M3, Canada

⁴Department of Construction Engineering, École de technologie supérieure, Montréal, QC H3C 1K3, Canada

⁵CentrEau, the Québec Water Management Research Centre, Québec City, QC GV1 0A6, Canada

10 *Correspondence to:* Vasana Dharmadasa (vasana.sandamali.dharmadasa@uqtr.ca)

Abstract. Accurate knowledge of snow depth distributions in forested regions is crucial for applications in hydrology and ecology. Understanding and assessing the effect of vegetation and topographic conditions on the snow depth variability is useful for the accurate prediction of snow depths. In this study, the spatial distribution of snow depth in two agro-forested sites and one coniferous site in eastern Canada was analyzed for topographic and vegetation effects on snow accumulation. Spatially distributed snow depths were derived by Unmanned Aerial Vehicle Light Detection and Ranging (UAV-lidar) surveys conducted in 2019 and 2020. Distinct patterns of snow accumulation and erosion in open areas (fields) versus adjacent forested areas were observed in lidar-derived snow depth maps at all sites. Omnidirectional semi-variogram analysis of snow depths showed the existence of a scale break distance less than 10 m in the forested area at all three sites, whereas open areas showed scale invariance or comparatively large scale break distances (i.e., 18 m). The effect of vegetation and topographic variables on the spatial variability of snow depths at each site was investigated with random forest models. Results show that including wind-related forest edge proximity effects improved the model accuracy by more than 50 % in agro-forested sites, whereas incorporating canopy characteristics improved the model accuracy by more than 60 % in the coniferous site. Hence the underlying topography and the wind-redistribution of snow along forest edges govern the snow depth variability at agro-forested sites, while forest structure variability dominates snow depth variability in the coniferous environment. These results highlight the importance of including and better representing these processes in process-based models for accurate estimates of snowpack dynamics. This study also demonstrates the usefulness of UAV-lidar to resolve and understand high-resolution snow depth heterogeneity in agro-forested environments and boreal forests.

1 Introduction / problematic

Knowledge of spring snowpack conditions is essential to accurately estimate water availability and flood peaks following the onset of melt (Hopkinson et al., 2004). Many studies showed that addressing the spatial distribution of snow depth prior to melting is more important than spatial differences in melt behavior when estimating melt dynamics of the snowpack (e.g.,



Schirmer and Lehning, 2011; Egli et al., 2012). Evaluating snowpack conditions in forested regions is particularly crucial as the forest cover significantly modifies snow accumulation and ablation processes due to canopy interception and changes energy balance processes within the canopy. These changes produce a marked effect on the downstream hydrograph (Roth and Nolin, 2017). In addition, forests can also influence the differential snow accumulation by preferential deposition of wind-blown snow along the forest edges (Essery et al., 2009; Currier and Lundquist, 2018).

Spatial variability of the snow cover is mainly controlled by topography and vegetation type, and density (Golding and Swanson, 1986; Jost et al., 2007; Varhola et al., 2010a; Koutantou et al., 2022). With the advent of remote sensing techniques, airborne (piloted and unpiloted) laser (lidar: light detection and ranging) scanning techniques have been extensively used to monitor snowpacks due to their strong penetration ability through the canopy to detect underlying snow cover/ground (Hopkinson et al., 2004; Morsdorf et al., 2006; Hopkinson et al., 2010; Harpold et al., 2014; Zheng et al., 2016; Currier and Lundquist, 2018; Zheng et al., 2018; Mazzotti et al., 2019; Harder et al., 2020; Jacobs et al., 2021). Lidar scanning also typically allows capturing high-resolution micro (<100 m) and mesoscale (100 m–10 km) variability and allows producing high resolution (<10 m) snow depth/cover maps.

Snow spatial variability can occur on more than one scale due to different processes acting over multiple scales (Deems et al., 2006). Several studies emphasized a multiscale behavior of snow depths with two distinct regions (scales) separated by a scale break at a location varying from meters to tens of meters, with a more strongly spatially correlated snow depth structure before the scale break (Deems et al., 2006; Fassnacht and Deems, 2006; Trujillo et al., 2007; Deems et al., 2008; Trujillo et al., 2009; Mott et al., 2011; Schirmer and Lehning, 2011; Mendoza et al., 2020). In turn, this suggests the existence of different processes controlling the snow accumulation, and distribution over these two distinct scales. For instance, these studies emphasized that a short scale break distance in forested areas (9–12 m) is reflected by canopy interception where the effect of wind redistribution is minimal (Deems et al., 2006; Trujillo et al., 2007). Comparatively a longer distance (15–65 m) in tundra regions is reflected by the interaction of wind, vegetation, and terrain roughness (Trujillo et al., 2009), while a shorter (6 m) and longer (20 m) distance in non-vegetated areas are explained by the interaction of the wind with terrain roughness in sheltered and exposed mountain slopes respectively (Mott et al., 2011; Schirmer and Lehning, 2011). The knowledge of this scale break location is important to choose the resolution required for remotely sensed or in situ data collection efforts in order to represent the snowpack variability at different scales.

In addition to the scaling properties of snow distribution, the relationships between snow depth, topography, and forest structure are also an important aspect in understanding/assessing small-scale snow heterogeneity in forested environments. The need to quantify these complex relationships has inspired the development of modeling approaches like empirical models (e.g., Anderton et al., 2004; Winkler et al., 2005; Grünwald et al., 2013) and process-based models (e.g., Hedstrom and Pomeroy, 1998; Liston and Elder, 2006). While process-based models are applicable to a wide range of conditions, they do require an extensive amount of input data. Contrarily, empirical models are useful in establishing a general relationship between the variables and provide a first-order estimate of their effects on snow processes. However, they do not explicitly account for governing processes, and thus may not make accurate predictions under specific conditions (Varhola et al.,



2010a). Nevertheless, the use and effectiveness of empirical models like multiple linear regressions (MLR) (Jost et al., 2007; Lehning et al., 2011; Grünewald et al., 2013; Revuelto et al., 2014; Zheng et al., 2016; Zheng et al., 2018) and binary regression trees (BRT) (Elder et al., 1995; Elder et al., 1998; Winstral et al., 2002; Anderton et al., 2004; Molotch et al., 2005; Baños et al., 2011; Revuelto et al., 2014) to relate snow depth/SWE patterns with terrain and land cover predictors is well documented. Compared to linear methods, tree-based methods have the ability to describe more complex and nonlinear relationships between snow depth and the independent variables (Erxleben et al., 2002; Veatch et al., 2009; Bair et al., 2018). In recent years, the random forest (RF) model, an ensemble machine learning algorithm that combines several randomized decision trees and aggregates their predictions, started gaining popularity in water science and hydrological applications (Tyrallis et al., 2019). The use of the ensemble bagging approach in RF models reduces overfitting, which is a well-known issue with traditional decision trees, and provides more accurate and unbiased error estimates (Breiman, 2001). As yet, there is only a handful of studies that used RF models to estimate snow depths/SWE (Bair et al., 2018; Yang et al., 2020) other than those that used RF algorithm to express the relative importance of predictor variables (Zheng et al., 2016) or to predict spatially distributed lidar vertical errors (Tinkham et al., 2014).

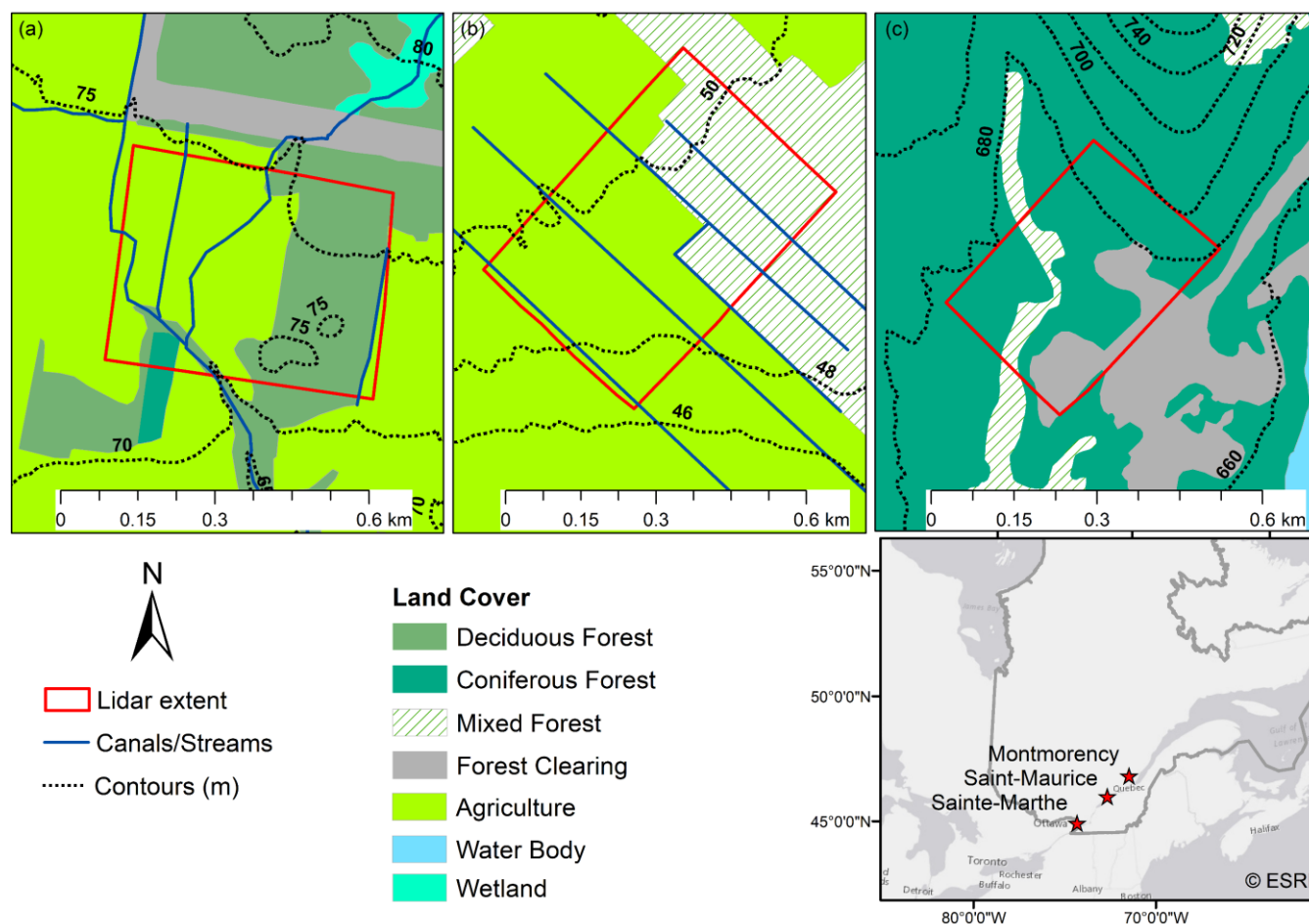
To our knowledge, to date, there are only a few previous studies that estimated snow depths by unpiloted aerial vehicle (UAV) based lidar (Harder et al., 2020; Cho et al., 2021; Jacobs et al., 2021; Koutantou et al., 2021; Dharmadasa et al., 2022; Koutantou et al., 2022; Proulx et al., 2022). None of them explicitly examined how terrain and vegetation characteristics influence the snow heterogeneity in different landscapes. From previous studies, Koutantou et al. (2022) successfully used UAV-lidar data on two opposing slopes with a heterogeneous forest cover at a high spatio-temporal scale to show the effect of canopy structure and solar radiation on snow dynamics excluding the effect of microtopography. The main objective of this paper is to study the small-scale spatial variability of snow depth by UAV-lidar and investigate the terrain and vegetation controls on this snow depth heterogeneity in an agro-forested and a boreal landscape. The study sites are based in southern Québec, Canada, where forests intertwined with mosaics of open agricultural fields in low-lying lands (agro-forested landscapes) play a significant role in altering the spatial distribution of the snow cover (Aygün et al., 2020). Much uncertainty still exists about the micro and meso scale spatial variability of snow cover and associated hydrological processes in these landscapes, partly due to lack of detailed and simultaneous micrometeorological and snowpack observations (Brown, 2010; Sena et al., 2017; Valence et al., 2022). To our knowledge, there has been no application of UAV laser scanning to investigate the small-scale snow cover heterogeneity in this type of landscape. As well, this paper provides some of the earliest results of snow depth mapping by UAV-lidar. This study will specifically explore: (1) how the snow accumulation and its scaling characteristics vary between and within forested and open environments, and (2) the relationship between snow depth, topography, and forest structure.



2 Data and methods

2.1 Study sites

Small-scale snow depth heterogeneity was investigated at three selected sites that represent the typical landscape in southern Québec (Fig. 1). Of the three sites, Sainte-Marthe and Saint-Maurice are agro-forested sites located in the St. Lawrence River lowlands. Irrigation canals and streams flowing through the open agricultural areas are very common in these agro-forested landscapes. The main crop type in the agricultural areas is soya. The forested area in Sainte-Marthe consists of a dense deciduous forest with sugar maple (*Acer saccharum*), red maple (*Acer rubrum*), and a small conifer plantation to the Southwest. Saint-Maurice has a high to moderate dense mixed forest with poplar (*Populus x canadensis*), red maple, white pine (*Pinus strobus*), and balsam fir (*Abies balsamea*) being the dominant tree species. Forêt Montmorency (hereafter Montmorency) is a dense boreal forest with balsam fir, black spruce (*Picea mariana*), and white spruce (*Picea glauca*) tree species farther north on the Canadian Shield. Forest gaps associated with clear-cutting and regeneration practices are common in this area. Adjacent to the forest is an open area hosting the NEIGE-FM snow research station, which hosts a variety of precipitation gauges and snowpack measuring sensors, and is part of the World Meteorological Organization's (WMO) (Royer et al., 2021). Table 1 summarizes the physiographic and climatic conditions at each site. Land use information presented in Fig.1 was obtained from the Québec Ministry of Forests, Wildlife, and Parks (MFFP). For the interpretation purpose, open agricultural areas in Sainte-Marthe and Saint-Maurice and the small open area in Montmorency (NEIGE-FM site) are referred to as "field" herein.



115 **Figure 1.** Overview of the study sites with lidar extents. (a) Sainte-Marthe, (b) Saint-Maurice and (c) Montmorency. Contour intervals intentionally differ between sites for better readability. (Adapted from the data from MFFP)

Table 1. Site characteristics and lidar data collection information

	Sainte-Marthe	Saint-Maurice	Montmorency
Elevation range, m	70–78	46–50	670–700
MAAT, °C	6.0	4.7	0.5
Total precipitation, mm/ y	1000	1063	1600
Snowfall/Total Precipitation, %	15	16	40
Winter season	November–March	November–March	October–April
Lidar extent, km ²	0.22	0.25	0.12
Forest area/Total area, %	40	40	92
Forest type	Deciduous	Mixed	Boreal



Mean canopy density, %	>80	60–80	60–80
Snow-on flight date	12 March 2020	11 March 2020	29 March 2019
Snow-off flight date	11 May 2020	02 May 2020	13 June 2019

MAAT= mean annual air temperature. Climatic data presented here were based on the climate averages (1981–2010) at the nearest Environment and Climate Change Canada (2021a) meteorological stations to the sites (Station climate ID 7016470, 7017585, and 7042388 for Sainte-Marthe, Saint-Maurice and Montmorency).

2.2 Data processing

All lidar surveys were performed with a GeoMMS system mounted onto a DJI M600 Pro UAV platform. The GeoMMS system is comprised of a Velodyne VLP-16 lidar sensor, a real-time dual-antenna global navigation satellite system (GNSS) aided inertial navigation system (INS) for precise heading, and a tactical MG364 inertial measurement unit (IMU). The nominal accuracy of the point cloud provided by GeoMMS is ± 5 cm (RMS, root mean square) (Geodetics, 2018) whereas the nominal uncorrelated relative error of two lidar point clouds is approximately ± 7 cm ($\sqrt{5^2 + 5^2}$). Flight paths for the surveys were prepared in UgCS flight control software (Sph-Engineering, 2019) and the flight parameters were optimized to reduce overall INS errors and maximize the mapping efficiency in the forested areas. Table 2 outlines the flight parameters and equipment settings used in surveys.

Raw lidar data sets collected from the flights were post-processed in Geodetics LiDARTool (Geodetics, 2019) with post-processing kinematic (PPK) correction. The PPK option regenerated a significantly more accurate trajectory file by combining the onboard GNSS data with GNSS base station data. Then, this post-processed trajectory file was merged with the raw laser data to produce a geo-referenced x,y,z point cloud. Noise removal was applied next. We also employed a trial-and-error, manual boresight calibration method to correct for boresight errors in the data, as recommended by the manufacturer (Geodetics, 2019). The final post-processed point clouds have an absolute accuracy range of 3–6 cm and a relative accuracy range of 4–6 cm (Dharmadasa et al., 2022).

To classify the bare surface points, we used the multiscale curvature algorithm (Evans and Hudak, 2007) implemented in the commercial Global Mapper software (Blue Marble Geographics, 2020). Parameters of the algorithm were adjusted according to the vertical spread of the flight strips over open terrain, the local slope of the terrain and canals/streams, and the presence/absence of buildings. The reader is referred to Dharmadasa et al. (2022) for a comprehensive overview of the UAV-lidar system and post-processing of raw data.



Table 2. Flight parameters and equipment settings

Flight parameters		Equipment settings	
Flying speed	3 m s ⁻¹	Wavelength	905 nm
Flight altitude	40 m AGL	Laser pulse repetition rate	18.08 kHz
Field of view (horizontal)	145°	Field of view (vertical)	±15°
Distance between parallel flight lines	64 m	Laser RPM	1200
Ground overlap	20 %	Return type	Dual
Point density	603 points m ⁻²		

2.2.1 Snow depth maps

150 Snow depth maps were quantified by differencing winter (snow-on) and summer (snow-off) digital elevation models (DEMs) generated from bare surface points at each site. Bare surface points were aggregated to a grid resolution of 1.4 m using the binning method in Global Mapper (Blue Marble Geographics, 2020). This grid resolution was selected based on the manual snow depth sampling strategy used by Dharmadasa et al. (2022) to validate the snow depth maps (five snow depth measurements were taken at each sampling location in a diagonal cross shape at 1 m apart, and the average of these

155 five measurements was considered to represent a $1.4 \times 1.4 \text{ m} (\sqrt{1^2 + 1^2})$ grid cell) and aimed to minimize the effect of positional errors of the manual measurements made with GNSS. As final filtering, spurious negative snow depths were set to zero, as they are physically inconsistent and need to be filtered (Hopkinson et al., 2012). Negative snow depths accounted for a very small portion of the total area (<0.1 %) sampled and had a negligible effect on the statistics derived from the snow depth maps. The validation of UAV-lidar snow depths with manual measurements showed a RMSE of 0.079–0.160 m in the

160 deciduous forested environment, and 0.096–0.190 m in the coniferous forested environment (Dharmadasa et al., 2022), which is comparable to previous efforts with UAV-lidar (Harder et al., 2016; Jacobs et al., 2021) and airborne lidar (Harpold et al., 2014; Painter et al., 2016). When taking into account the 2–10 cm thick ice layer that was typically observed at the base of the snowpack in the deciduous environment which limited the penetration of the snow depth manual probe into the soil, and the positional errors due to the multipath effect in the coniferous environment, our UAV-lidar snow depths maps

165 were deemed to be robust and to represent an improvement over previous studies. As well, the higher RMSE in the coniferous forested environment has a comparatively smaller impact due to the deeper snowpack observed at the site, i.e., the relative RMSE error (RMSE/mean snow depth) in the coniferous forested environment (0.068–0.135) is much lower than the relative error (0.321–0.420) in the deciduous forested environment where the snowpack is shallower. More details about the snow depth validation can be found in Dharmadasa et al. (2022).



170 2.2.2 Terrain metrics

To typify the terrain characteristics, we derived four variables from the summer DEM, i.e., elevation (*Elevation*), slope (*Slope*), aspect (*Aspect*), and topographic wind sheltering index (*TWSI*). Topographic variables other than elevation need to be considered when studying areas that encompass a small elevation range (Zheng et al., 2016), such as our sites. *Elevation* was obtained directly from the DEM, while *Slope* and *Aspect* were derived using ArcGIS 10.2 software. *Slope* was calculated as the first derivative of the DEM, while *Aspect* was derived in two orthogonal components, i.e., west-east (*Aspect_WE*) and south-north (*Aspect_SN*) exposures. *Aspect_WE* (west-negative, east-positive) and *Aspect_SN* (south-negative, north-positive) were calculated directly as the sine and cosine of the aspect, respectively. The *TWSI* was produced using the RSAGA package in CRAN. This variable considers the sheltering effects of the local topography in the dominant wind direction. Several studies showed that *TWSI* is a good measure to characterize sheltering and exposure of the local terrain which gives a reasonable representation of the local wind field and thus the redistribution of snow by wind (Winstral et al., 2002; Winstral and Marks, 2002; Plattner et al., 2004; Molotch et al., 2005). Negative *TWSI* values correspond to terrain exposure and positive values to sheltering from the wind. Dominant wind directions were extracted from the hourly wind data for the period 2019–2021 at each site (Fig. 2). Wind data was collected from an automatic weather station located 1.4 km away from the Sainte-Marthe site and the closest Environment Canada wind measuring stations at the other sites. The closest station to Saint-Maurice (climate ID 7018561) was 19 km away from the site and 0.25 km away from the Montmorency site (climate ID 7042395) (ECCC, 2021b).

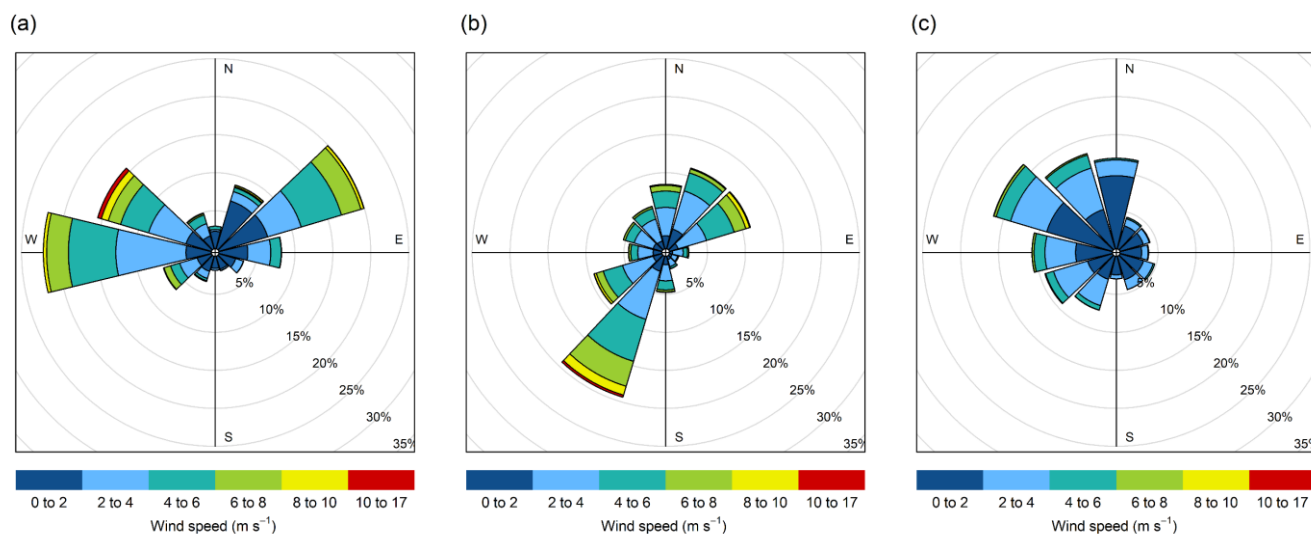


Figure 2. Wind rose plots of the sites. (a) Sainte-Marthe, (b) Saint-Maurice and (c) Montmorency

2.2.3 Vegetation descriptors

190 Vegetation-related variables were rasterized from the classified winter point cloud in LiDAR360 (Greenvalley-International, 2020). The forestry module of LiDAR360 contains tools that allow users to calculate essential forest metrics and accurately



195 extract individual tree parameters like crown diameter, crown area, and tree diameter by breast height from airborne lidar data. In this study, the leaf area index (*LAI*), canopy cover (*CC*), and gap fraction (*GF*) were estimated for the forest cover higher than 2 m. A 2 m height threshold was selected as canopies >2 m have been shown to have a strong influence on snow accumulation (Varhola et al., 2010b; Zheng et al., 2016; Zheng et al., 2019). The function used to calculate *LAI* is based on the Beer-Lambert law (Richardson et al., 2009). The estimated *LAI* is contingent on the average scan angle, *GF*, and the extinction coefficient. *GF* is calculated as the total number of ground points to the total number of lidar points within a grid cell. *CC* is calculated as the total number of vegetation returns to total returns (Morsdorf et al., 2006). Refer to Richardson et al. (2009) and Morsdorf et al. (2006) for the equations used to estimate the forest metrics. In addition, canopy height (*CH*) was derived by subtracting the DEM from the digital surface model (DSM). For rasterizing, a grid cell size slightly larger than the maximum individual crown diameter was selected to ensure that at least one tree was present within a grid cell (Li et al., 2012; Greenvalley-International, 2020). Grid resolutions obtained using this method were 20, 15, and 10 m in Sainte-Marthe, Saint-Maurice, and Montmorency, respectively.

2.2.4 Forest edge descriptors

205 We investigated forest edge effects on snow accumulation using an approach inspired from Currier and Lundquist (2018) using Matlab software. Analogous to their analysis, we added directionality to forest edges to examine if preferential snow accumulation occurred windward or leeward of forest edges due to snow redistribution by wind or reduced ablation due to shading from the forest. Pixels were first classified as north-facing (*NFE*) when they were within a maximum search distance d_{max} northward of the forest edge. Based on previous results by Currier and Lundquist (2018), d_{max} was set to 2H, where H is the typical tree height derived from the 1.4 m resolution canopy height model at each site. H is 15 m in Sainte-Marthe, 20 m in Saint-Maurice, and 12 m in Montmorency. A tolerance of $\pm 45^\circ$ was used for the search direction for *NFE*. Pixels were classified as windward (*WFE*) and leeward (*LFE*) when they were within a maximum search distance of the forest edge in the dominant wind direction. A range of search directions was used to constrain the dominant wind directions at each site, based on wind roses (Fig. 2). Two dominant wind cones, $270 \pm 15^\circ$, and $50 \pm 15^\circ$ were used in Sainte-Marthe, and one dominant wind cone in Saint-Maurice ($210 \pm 15^\circ$) and Montmorency ($310 \pm 15^\circ$). d_{max} was initially varied between 6–10H for pixels in open terrain based on Currier and Lundquist (2018) which represents the typical length scale of preferential snow accumulation at the forest edge. After a few trials, a final value of 10H was retained, which showed the highest correlation with snow depth. Moreover, the 10H distance at each site (150 m, 200 m, and 120 m in Sainte-Marthe, Saint-Maurice, and Montmorency respectively) encompassed the preferential snow accumulation seen along the forested edges on the lidar-derived snow depth maps. A maximum search distance of 1H was used for pixels within the forest in order to detect if preferential accumulation from blowing snow penetrated the forest. This value was chosen based on visual observations in the field, which suggested limited penetration of blowing snow inside the forest. A novel index of proximity to the forest edge, *FE*, was calculated by scaling the distance between each pixel and the forest edge (d) by the maximum search distance, d_{max} :



$$FE = \frac{d_{max} - d}{d_{max}} \quad (1)$$

225 *FE* (either *NFE*, *WFE*, or *LFE*, depending on the initial classification) is equal to one when a pixel is situated on the forest edge and equal to zero when it is located at, or beyond the maximum search distance d_{max} . The novelty of this approach is to derive a continuous predictor of forest edge proximity, as opposed to the simpler binary classification introduced by Currier and Lundquist (2018).

2.3 Data analysis

230 Data analysis was primarily focused on assessing the small-scale snow depth heterogeneity at the selected sites. Lidar-derived snow depth data were analyzed for inter (agro-forested versus coniferous) and intra (field versus forest) site variability. First, the scale dependence of snow depth variability was explored using semi-variogram analysis. Then, the site-specific topographic and vegetation control on the snow depth spatial heterogeneity was examined with RF regression models. All the statistical analyses were performed in R software.

235 2.3.1 Spatial correlation analysis

To analyze the small-scale spatial variability of the snow depth map in each study site, omnidirectional semi-variograms were used. Semi-variogram analysis allows constraining the dominant scales of snow depth variability and to compare them between land cover types and sites. Canals/streams were discarded from the snow depth maps for this analysis to ensure stationarity of the surface. i.e., snow depths in canals/streams would have a unidirectional spatial correlation which could alter the relationship of the overall terrain by introducing biases. The semi-variogram $\gamma(r)$ is expressed as:

$$\gamma(r_k) = \frac{1}{2N(r_k)} \sum_{(i,j) \in N(r_k)} \{z_i - z_j\}^2 \quad (2)$$

Where r is the lag distance of bin k , $N(r_k)$ is the total number of pairs of points in the k^{th} bin and z_i and z_j are the snow depth values at two different point locations i and j (Webster and Oliver, 2007).

We used 50 log-width bins for the semi-variogram analysis. Log-width distance bins provide equal bin widths when semi-variograms are transformed to log-log scale, and help resolve the variogram at short length scales by allowing greater bin density at shorter lag distance compared to linear-width bins (Deems et al., 2006).

In the case of scale invariance, the variogram can be described by a power law:

$$\gamma(r) = ar^b \quad (3)$$

Where a and b are coefficients selected to minimize the squared residuals.

2.3.2 Random forest model

To investigate the effect of vegetation and topographic variables on the spatial variability of snow depth, we applied RF regression models on the rasters derived from lidar data. Generally in a RF model, two-thirds of the sample data (in-bag) is



used to train the model, while the remaining one-third (out-of-bag, OOB) is used to estimate how well the trained model performs (as a validation set). These OOB observations are used to calculate predictor importance, which shows the relative contribution of each predictor (independent) variable to the response variable.

To have a consistent grid resolution in the analysis, the snow depth, terrain metrics, and *CH* were aggregated to the grid resolution of the vegetation descriptors. Thus, the analyses were conducted with grid resolutions of 20 m, 15 m, and 10 m in Sainte-Marthe, Saint-Maurice, and Montmorency, respectively. Apart from the derived variables mentioned in section 2.2, a binary variable (*Site*) representing forested (1), and field (0) pixels was included in the regression analysis to investigate systematic effects, if any, of land cover that was not captured by vegetation or terrain metrics. As a precautionary measure, we also excluded collinear variables prior to building the RF models using the variance inflation factor (VIF) function in R. This was done mainly because our objective was to investigate the relative contribution of different variables to snow depth variability in forest versus the field, rather than deriving a model with maximum predictive capacity. While RF can handle collinearity in a predictive mode, collinearity makes it difficult to separately evaluate the predictive power (variable importance) of the predictors (Bair et al., 2018). The number of trees in the ensemble (*ntree*) and the number of variables at each node (*mtry*) were optimized for each RF model. RF model results are first presented according to the relative importance of predictor variables (variable importance plots), which has proven to be useful for evaluating the relative contribution of input variables (Tyrallis et al., 2019). The value of the variable importance of a variable reflects how much removing this variable would decrease the accuracy of the model and vice versa. Then the partial relationships of the variables with the snow depth were examined and presented. Finally, the performance of RF models in terms of validation statistics (OOB) was compared between different land cover types and sites.

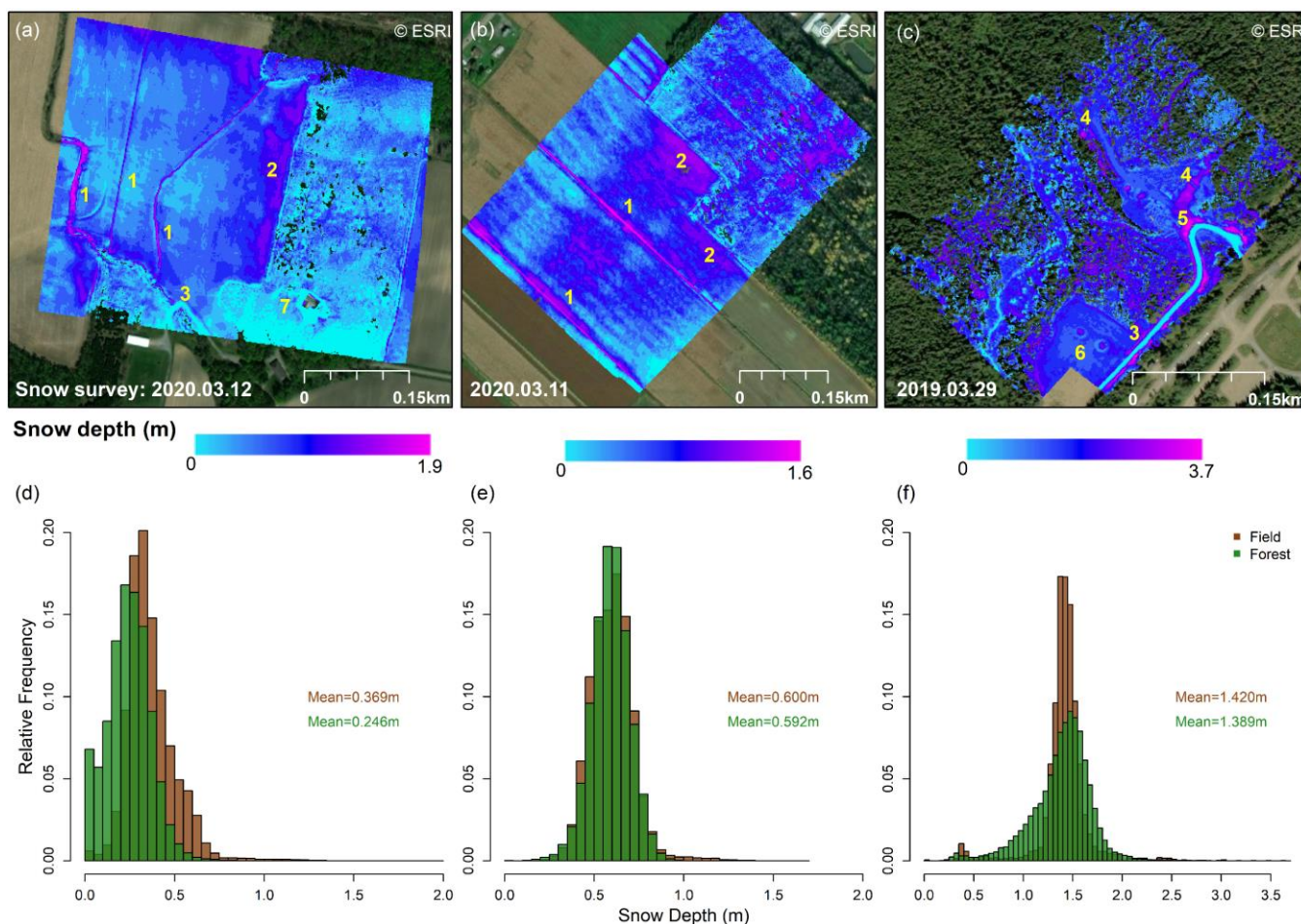
3 Results

3.1 General snow accumulation patterns

Figure 3 depicts the snow depth maps derived from UAV-lidar data at the study sites. Montmorency shows the highest overall snow accumulation with a maximum of 3.7 m. Higher snow accumulation in canals/streams (area 1 in Fig. 3a, b) and along the forest edge (area 2 in Fig. 3a, b) is evident in Sainte-Marthe and Saint-Maurice, whereas in Montmorency, forest gaps (area 4 in Fig. 3c) seem to accumulate more snow. The highest snow depth in Montmorency corresponds to localized, artificial snow piles adjacent to the main road as observed during the field campaign (area 5 in Fig. 3c). Concentric snow accumulation patterns around the double fence precipitation gauges are also noticeable in Montmorency snow depth map (area 6 in Fig. 3c). Compared to the other two sites, the Montmorency snow depth map comprises more data gaps in the forested area. Paved roads in Sainte-Marthe (area 3 in Fig. 3a) and Montmorency (area 3 in Fig. 3c) and the area surrounding the small house (area 7 in Fig. 3a and Fig. 3d) in the forest at Sainte-Marthe appear snow-free due to the snow clearing operations, as confirmed in field campaigns. Snow clearing in the proximity of the house in Sainte-Marthe accounts for a significant portion of zero and/or small snow depths (Fig. 3d) and biases the mean snow depth in the forest. When this



285 portion is discarded, the mean snow depth in the forest increases from 0.246 to 0.275 m. Hence in Sainte-Marthe, the mean snow depth in the field area is higher than that in the adjacent forested area (Fig. 3d), whereas, at the other two sites, mean snow depths in the field and forest are similar considering the measurement error of the lidar system (Fig. 3e, f). Although the maximum snow depth is higher in Sainte-Marthe (1.9 m) compared to Saint-Maurice (1.6 m), snow depths in Sainte-Marthe (0.246–0.369 m) appear to be lower on average than in Saint-Maurice (0.592–0.600 m).



290 **Figure 3.** UAV-lidar derived snow depth maps (grid size 1.4 m) and histograms of snow depth distribution. (a, d) Sainte-Marthe map with snow surveying date and histogram; (b, e) Saint-Maurice map with snow surveying date and histogram; (c, f) Montmorency map with snow surveying date and histogram. Features 1 to 7 are discussed in the text.

3.2 Spatial correlation analysis

295 Omnidirectional semi-variograms of snow depth at the study sites are shown on a log-log scale in Fig 4. Semi-variograms were discretely developed for field and forested areas to assess the effect of landcover on the snow depth variability. Overall, forested areas show more variable (higher semi-variance values) snow depths than field snow depths at all sites. Snow depths seem to be more variable in the coniferous forest than in deciduous and mixed forests. Forested areas at all three sites



show a typical multifractal behavior, where the semi-variance between neighboring snow depths increases rapidly up to a scale break located at distances less than 10 m (Fig. 4), followed by a slower increase after. The Sainte-Marthe field area does not exhibit a distinct scale break. In contrast, both Saint-Maurice and Montmorency field areas show multiscale
300 behavior.

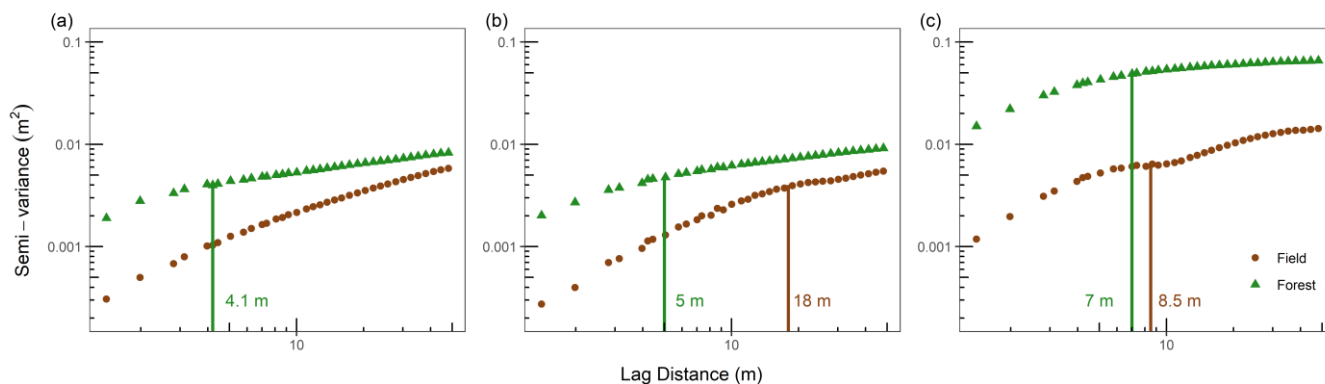


Figure 4. Omnidirectional semi-variogram for the field and forested areas at (a) Sainte-Marthe, (b) Saint-Maurice and (c) Montmorency. Vertical lines indicate the dominant scale breaks.

3.3 Random forest analysis

305 3.3.1 Potential predictors of RF model

We discarded *Elevation* from the analysis since the elevation difference at any of the three sites was too small (Table 1) to produce any meaningful local orographic effect on precipitation, or adiabatic effects on air temperature, e.g., Mazzotti et al. (2019). As well, *LFE* was found to have a negligible influence on snow depth, hence was also excluded from the list of potential predictors. *CC* and the binary *Site* variable were further excluded due to collinearity issues. Collinearity analysis
310 suggested discarding *GF* and *CH* in favor of *LAI* at the two agro-forested sites, while *LAI* was instead flagged as colinear instead of *GF* and *CH* in the coniferous site. Since *LAI*, *GF* and *CH* are strongly intercorrelated ($r = 0.84\text{--}0.97$), and because *LAI* has been shown to be a strong predictor of snow accumulations in forests (Hedstrom and Pomeroy, 1998; Pomeroy et al., 1998; Broxton et al., 2015; Lendziuch et al., 2016) we chose to retain *LAI* as a common forest metric and discard *GF* and *CH* to allow for a better intercomparison of the snow depth variability with vegetation across all three sites. The final
315 potential predictor variables retained for all three sites were *Slope*, *Aspect_WE*, *Aspect_SN*, *TWSI*, *LAI*, *WFE*, and *NFE*.

3.3.2 Relative importance of topography and vegetation on snow depth variability

The relative importance of predictor variables in Fig. 5 summarizes the relative contribution of the different topographic, vegetation, and forest edge effects on snow depth spatial variability at each site. The windward forest edge proximity (*WFE*) has the strongest influence on snow depth variability in both Sainte-Marthe (50 %) and Saint-Maurice (76 %) when both
320 landscape units (field+forest) are combined, and the north-facing forest edge proximity index (*NFE*) has the least influence



(12 % and 10 %). In Montmorency, *LAI* and *WFE* respectively have the highest (64 %) and least (3 %) impact on snow depth variability for the combined landscape unit. The importance of variables somewhat changes when forests and fields are modelled independently, implying different dominant factors/processes acting in forests and fields. For instance, in Sainte-Marthe, the northern exposure (*Aspect_SN*) seems to be the dominant variable (31 %) for snow depth variability in the forest
 325 followed by *TWSI* (28 %), *Slope* (22 %), and *LAI* (17 %). In Sainte-Marthe field, *WFE* (58 %), *Slope* (25 %), and *TWSI* (25 %)
 are the most important variables. *WFE* (13 %), *TWSI* (13 %), and *LAI* (6 %) have the highest influence on snow depth within the Saint-Maurice forest whereas in the adjacent field *WFE* (69 %), *TWSI* (39 %), and *Slope* (33 %) predominate. The importance of *LAI* (73 %), *TWSI* (28 %), and *Aspect_WE* (20 %) is higher for snow depths within the coniferous forest with gaps in Montmorency, whereas the snow depths in the small field are mostly influenced by *NFE* (15 %), *Aspect_SN* (12 %),
 330 and *LAI* (9 %).

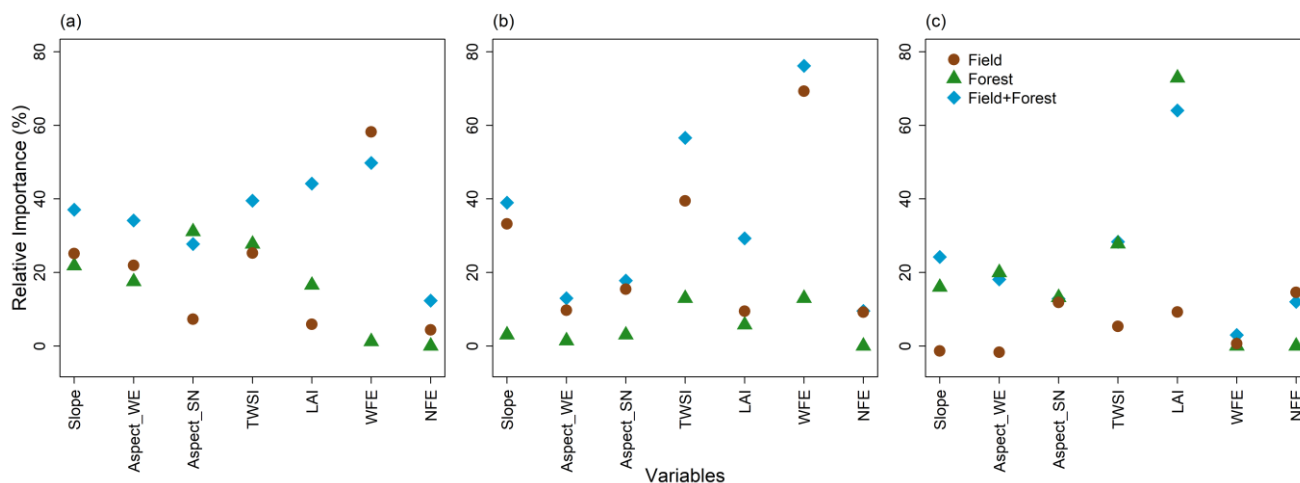


Figure 5. Relative importance of variables in predicting snow depths. (a) Sainte-Marthe, (b) Saint-Maurice and (c) Montmorency.

3.3.3 Partial relationships of predictor variables with snow depth

As seen in Fig. 6, all variables exhibit a non-linear relationship with snow depth across all sites. Note that the positive *LAI*
 335 values in field areas correspond to a few isolated *LAI* pixels along the forest edges, the boundary between field and forest.
 The following sections describe the results obtained at each site.

Sainte-Marthe

The mild slopes of this site do not show a strong relationship with snow depths in field+forest and forest, but field snow
 340 depths show a slight increase at higher slopes (Fig. 6a). There is no apparent preferential accumulation of snow on either
 west or east-facing slopes (*Aspect_WE*). However, snow seems to accumulate preferentially on northern exposed slopes,
 especially within the forest (*Aspect_SN* graph in Fig. 6a). The general relationship of snow depth with *TWSI* suggests that
 increased topographic sheltering from the wind (increasing *TWSI* values), leads to higher snow accumulation. There is a



345 decrease in snow depths in response to increasing *LAI* for the combined field+forest and within the forest, though the relation is weak in the forest, with snow depth increasing up to a *LAI* of 0.5 which could reflect the forest edge transition, and decreasing afterward. Snow depth in the field and field+forest increases in response to increasing *WFE*, whereas snow depth in the forest does not show any significant change. *NFE* does not show a substantial effect on snow depths.

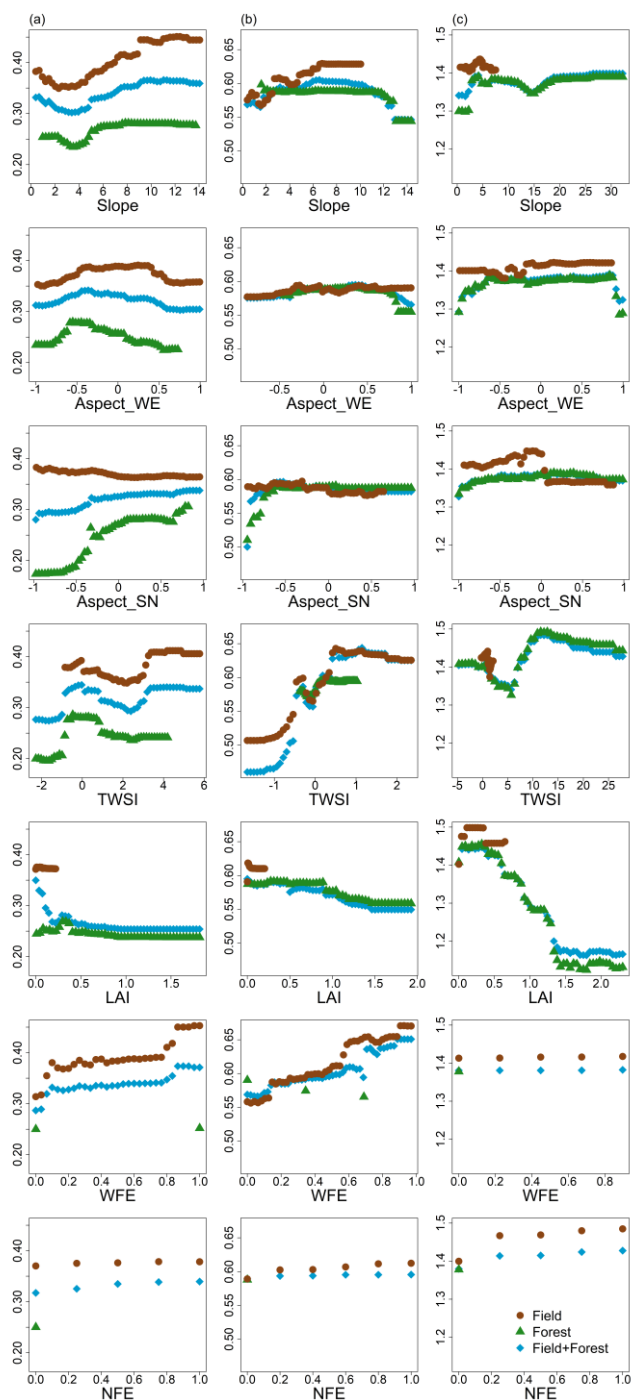
Saint-Maurice

350 Snow depths in Saint-Maurice (Fig. 6b) seem to increase with increasing slopes in the field while the reverse relationship is seen in the forest for higher slopes. There is a slight increase in snow depth from westerly to easterly slopes in the forest, ending with a sharp decrease for easterly slopes in the forest (*Aspect_WE*>0.5), due to fewer easterly pixels in the forest (Supplement Fig. S2). Field snow depths show a slight increase from west to east aspects but do not show any visible dependence on south-north aspects. Similar to Sainte-Marthe, snow accumulation in the forest is favored on northerly slopes.
355 Snow depth shows a general increase in response to increasing *TWSI*, with the greatest contribution to this relation from field snow depths. A non-linear decrease of snow depth with increasing *LAI*, stronger than that seen in Sainte-Marthe, is clearly visible in Saint-Maurice. However, contrary to Sainte-Marthe, the overall relationship is dominated by intra forest variations in *LAI* rather than the difference between the field and forest. Field and field+forest snow depths show a similar pattern to Sainte-Marthe with an increase in response to *WFE*. On the contrary, forest snow depth shows a slight decrease with
360 increasing *WFE*. However, snow depth in the field shows an increase in more northerly oriented forest edge pixels (*NFE*).

Montmorency

Slopes in the Montmorency forest (Fig. 6c) seemingly govern the overall snow depth-*Slope* relationship in this site. Snow depths increase linearly until *Slope* reaches $\sim 5^\circ$ and then remain nearly constant afterward. There is no apparent preferential
365 accumulation of snow on either west or east-facing slopes (*Aspect_WE*). Contrary to other sites, Montmorency forest does not show any preferential snow accumulation on northerly or southerly slopes, but field slopes with southern aspects seemingly accumulate higher snow depths than northern aspects. Forest *TWSI* appears to govern the overall snow depth-*TWSI* relationship, probably due to its larger extent compared to the other sites. The range of *TWSI* values in Montmorency, especially the positive (sheltering) ones, are much higher than in the other two sites, due to the more rugged topography in
370 Montmorency. The snow depth-*TWSI* relationship is complex, but generally shows a positive trend. This site shows a relationship of snow depth with *LAI* similar to the other sites, especially Saint-Maurice, with snow depth decreasing until *LAI* reaches ~ 1.5 . *WFE* does not show a considerable effect on snow depths in Montmorency. However, snow depth in the field shows an increase in more northerly oriented forest edge pixels.

375

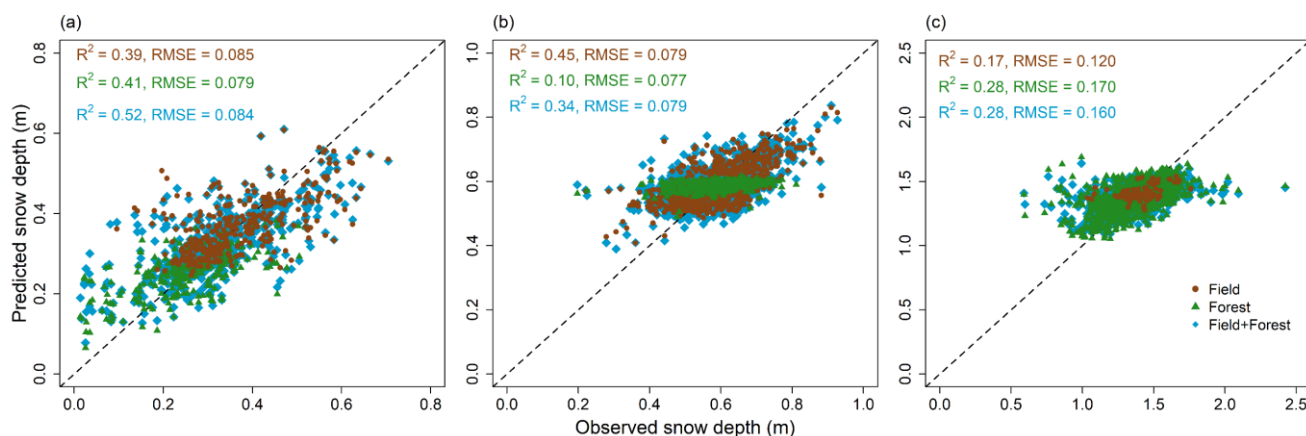


380 **Figure 6.** Partial relationship of predictor variables with snow depth. (a) Sainte-Marthe, (b) Saint-Maurice and (c) Montmorency. Predictor variables are presented by rows and sites by columns. Y axes represent the snow depth in m.



3.3.4 Performance of RF models at each site

Figure 7 displays the observed versus RF model estimates of the snow depth with corresponding OOB statistics for each site. Statistics are presented individually for the field, forest, and combined landscapes. Among the three sites, Sainte-Marthe RF model generally performs better with an OOB R^2 of 0.52 and RMSE of 0.084 m, and Montmorency shows the weakest performance with an R^2 of 0.28 and RMSE of 0.160 m. Sainte-Marthe field and forest models have similar R^2 and RMSE statistics (Fig. 7a), while Saint-Maurice field model performance is comparatively better (higher R^2 and lower RMSE, Fig. 7b) than that in the forest. On the contrary, Montmorency forest model performs better than that of the field (Fig. 7c).



390 **Figure 7.** RF model performance against observed snow depths. (a) Sainte-Marthe, (b) Saint-Maurice and (c) Montmorency. The stippled line depicts the 1:1 relationship.

4 Discussion

4.1 Spatial variability of forest versus field snow depths

Snow depths in Fig. 3 show a remarkable microtopographic variability across all sites. Our results in Sainte-Marthe underpin the previous finding that forested areas accumulate less snow than the adjacent open areas due to canopy interception and sublimation losses and sheltering from wind (Pomeroy and Granger, 1997; Hopkinson et al., 2004; Varhola et al., 2010a; Zheng et al., 2018; Hojatimalekshah et al., 2021). But other two sites show on average, a similar amount of snow accumulation in the field and forest. The dense coniferous canopy cover in Montmorency prevented laser shots from reaching the ground at some locations and consequently showed up as data gaps in the snow depth map (Fig. 3c). The snow depth patterns in the coniferous site thus appear to be dominated by canopy closure, i.e., forest clearings have higher snow depths than adjacent canopies. Such patterns have been previously reported by both ALS and UAV-lidar studies in western alpine/pre-alpine environments with different climates (Hopkinson et al., 2004; Zheng et al., 2016; Mazzotti et al., 2019; Jacobs et al., 2021).



In the agro-forested sites, comparatively higher snow depths observed in the open field compared to the adjacent forest patches are in contrast to what Aygün et al. (2020) observed in similar environments in southern Québec. They measured a lower snow accumulation in exposed agricultural fields (excluding the canals and the forest edge) compared to the adjacent deciduous and mixed forests. In our results, higher snow depth values at the two agro-forested sites principally correspond to canal/stream locations in the field and forest edges, which trap the snow blown from the open field with greater fetches. Hence canals/streams and forest edges constitute the main structuring elements of snow spatial variability at these sites. However, if canals and forest edge snow depths are discarded, agro-forested snow depth maps illustrate somewhat similar phenomena to Aygün et al. (2020), where snow depths in the exposed field appear to be slightly lower than those in the forest. Clusters of high snow depth values in the central area of the Saint-Maurice field in Fig. 3b could be due to local redeposition of snow by the wind in the microtopography or larger-scale effects. This could not be verified as unfortunately, the manual measurements in Saint-Maurice could not be retrieved due to a probe malfunctioning (Dharmadasa et al., 2022). Yet, the *TWSI* map (Supplement Fig. S2) suggests microtopographic wind sheltering could be the reason for the local snow deposition closer to the forest edge. But the probable cause for the other high snow depth cluster between two streams in the field could not be resolved from available data. However, as the canopy interception and losses in deciduous and mixed forests are expected to be small (Hopkinson et al., 2010; Aygün et al., 2020), the amount of differential snow depths between the open field and shaded forest would mostly depend on the amount of erosion in the field, and perhaps snowmelt losses in the field prior to peak snow accumulation. As well, a visual comparison of the inter-site snow depth maps suggests that the snow accumulation along the forest edges is a prime process in agro-forested landscapes.

4.2 Scaling characteristics of forest versus field snow depths

Semi-variogram analyses revealed distinct scaling behaviors in forest versus field snow depths (Fig. 4). Our results suggest a more variable (high semi-variance values) and more spatially continuous (larger scale break distance) snowpack in the Montmorency boreal forest compared to the temperate forest sites. The snowpack in the mixed forest at Saint-Maurice was less variable and more spatially continuous than that in the Sainte-Marthe deciduous forest. Compared to forested areas, the snowpack in field areas was less variable and more spatially continuous. Shorter scale break distances in forested areas compared to open field areas (Fig. 4) is analogous to previous studies that studied the fractal distribution of snow depths with lidar data. Previous studies reported scale break distances of 7–9 m for high to moderately dense coniferous forests (Trujillo et al., 2007; Trujillo et al., 2009), 12 m for a moderately dense deciduous forest (Trujillo et al., 2007; Trujillo et al., 2009), 15.5 m for a dense coniferous forest with open meadows (Deems et al., 2006; Fassnacht and Deems, 2006), and 16.5 m for a sparse coniferous forest (Deems et al., 2006; Fassnacht and Deems, 2006). We found the shortest scale break distance of 4.1 m for the dense deciduous forest in Sainte-Marthe, an intermediate distance of 5 m for the moderately dense mixed forest in Saint-Maurice, and a value of 7 m for the dense coniferous forest interspersed with gaps in Montmorency. These values are rather smaller than those reported by the previous studies. This could be due to inherent characteristics of the forests such as canopy density and size of open areas (gaps). It is also plausible that the dense point cloud provided by UAV (~150–600



points m^{-2} , (Zhang et al., 2019; Harder et al., 2020; Jacobs et al., 2021; Dharmadasa et al., 2022)) was able to resolve spatially distributed snow depth patterns at finer scales than that permitted by previous ALS surveys, which had typical point densities of $\sim 8\text{--}16$ points m^{-2} (Kirchner et al., 2014; Broxton et al., 2015; Broxton et al., 2019; Currier et al., 2019).

440 The relatively higher scale break distance in Montmorency forest could be due to the prevailing large gaps in the forest as a result of silvicultural practices and inherent efficient canopy interception of conifers. Coniferous trees have a substantial impact on snow depths as they intercept snow efficiently and unload around the crown (Zheng et al., 2019). Thus, a longer correlation length (at least the diameter of a tree crown) is expected as well as greater variability of snow depth in the coniferous environment compared to the more random deciduous tree structures which have reduced and more transient
445 snow storage. Leafless deciduous trees aid faster unloading of snow through branches as opposed to unloading around the crown in conifers and thus can result in a smaller correlation length in snow depth.

The largest scale break distance was found in the Saint-Maurice field (18 m). With the absence of vegetation in the field in winter and its high exposure to wind (Fig. 2b), this value is of similar magnitude to those reported for wind-exposed slopes in alpine environments by Schirmer and Lehning (2011), Mott et al. (2011), and Mendoza et al. (2020). Scale invariance in
450 the Sainte-Marthe field suggests a more spatially continuous snowpack. This interpretation is supported by the snow depth maps in Fig. 3, which show a smooth snow depth pattern that is only disrupted by preferential accumulation within irrigation canals/streams. The comparatively smaller scale break distance in the Montmorency field (8.5 m) could be due to its small extent and the influence of preferential accumulation near the meteorological equipment (concentric snow accumulations patterns around the two double-fenced precipitation gauges in Fig. 3c).

455 Generally, the scale break distances found in this study suggest that the scale selected for modeling or sampling in similar environments should be well below these values, in order to represent the small-scale variability of the snow depth.

4.3 Relationship of snow depth to topographic and vegetation characteristics

Our results affirm the non-linearity between snow depth and the variables considered and the importance of considering this non-linearity in statistical models. During the analysis, some consistent patterns emerged between all three sites, which have
460 been found in previous studies, i.e., snow depth generally decreases with an increase in *LAI* values (Varhola et al., 2010b), and snow depth increases with an increase of *TWSI* (Revuelto et al., 2014).

In the two agro-forested sites, field snow depth variability is governed by the preferential snow accumulation in canals/streams and the microtopography of the local terrain. In fact, the highest wind sheltering values were found in canals/streams which accumulated more snow (Fig. 3 and Supplement Fig. S1, S2). Within the forested areas, the influence
465 of forest structure (*LAI*) was not as strong as expected; instead, the influence of microtopography appeared to be governing the snow depth variability. The lower influence of *LAI* at these sites probably reflects the abundance of leafless trees in winter, which reduce interception losses and concurrent spatial snowpack variability. Moreover, the microtopography of these landscapes is closely related to the surficial geology of the sites. Preserved forested patches in the St. Lawrence River lowlands often correspond to less favorable soil conditions, such as glacial till and/or with bedrock outcrops and associated



470 rougher microtopography. Whereas agricultural fields are associated with glaciomarine or fluvio-glacial sediments that are
flatter in nature and exhibit even more flatter surface conditions because of machinery usage (MFFP, Québec Research and
Development Institute for the Agri-Environment (IRDA) and La Financière Agricole du Québec (FADQ)). Under limited
wind transport, this rougher microtopography in forested surfaces creates a directional bias that promotes lateral transport of
snow particles (bounce/ roll/ ejection) and therefore enhances the smoothing of the snow surface (Filhol and Sturm, 2019)
475 and dominates the snow heterogeneity within the forest. The absence of apparent preferential snow accumulation on
different slope orientations in agricultural fields suggests a smoothing of snow cover due to wind redistribution in the
field. More rugged microtopography of the forested soil seems to influence the snow cover through radiation resulting in
more snow accumulations on northerly slopes in the forest (Fig. 6a, b).

At the combined scale (field+forest), the agro-forested sites are dominated by blowing snow accumulation along the forest
480 edges (Fig. 5a, b). This effect is well visible on lidar-derived snow depth maps as well (Fig. 3a, b). Comparatively high wind
speeds and dominant wind directions (Fig. 2a, b) at these sites create favorable conditions for preferential deposition of
blowing snow at the forest edge due to the large expanses of open terrain upwind of the windward forest edges. Preferential
snow deposition by wind-induced snow drifting along the forest edge has been previously reported in alpine environments
by Veatch et al. (2009), Essery et al. (2009), Broxton et al. (2015), and Currier and Lundquist (2018). However, there seems
485 to be limited penetration of blowing snow inside the forest (*WFE* forest points in Fig. 6a, b).

Forest shading seemingly does not have a significant influence on the snow depth variability in these sites during the
accumulation season. Shading effects would however probably have some influence on snow depth patterns in the melting
season (Hojatimalekshah et al., 2021). This high spatial heterogeneity of snow depths and associated processes challenge the
distributed snow modeling using hydraulic response units (HRUs) in agro-forested landscapes (Aygün et al., 2020), where
490 HRUs are classified as field and forest patches but disregard boundary effects. Aygün et al., (2020) successfully modelled
blowing snow transport in fields and the preferential accumulation in canals and streams and assumed that once these were
filled, any further blown snow accumulated in the forest. Our results confirm the preferential accumulation in field canals
and streams but suggest that further blown snow first preferentially accumulates at the forest edge, which should eventually
be represented as distinct HRUs in distributed hydrological models of agro-forested landscapes.

495 The findings in agro-forested sites are in contrast with the boreal forested environment, where forest structure (*LAI*)
predominates on the variability of snow depth (Fig. 5 and Fig. 6). The small field appears to have fewer microtopographic
features and is mostly sheltered from the most frequent winds coming from the northwest direction (Fig. 2c). Relatively
greater positive *TWSI* values in this site imply more rugged microtopography and a larger degree of wind sheltering in the
forested terrain. However, since wind is mostly impeded by the coniferous trees, the *TWSI*-snow depth relationship in the
500 forest suggests that the snow displacement is driven by small-scale bounce/ejection/roll mechanisms, and preferential snow
deposition is driven by immobilizing mechanisms such as adhesion, cohesion, and physical interlocking of snow particles
(Filhol and Sturm, 2019) and unloading of snow by the canopy (Zheng et al., 2019). The lesser importance of *TWSI* (28 %
compared to 73 % of *LAI*, the dominant variable, Fig. 5) as a predictor in the coniferous forest compared to deciduous and



505 mixed forests, and the more or less constant snow depth values for slopes higher than 5° (Fig. 6c) suggest that microtopography has a more restricted influence on deeper snowpack at this site compared to the shallower snowpack at other sites. i.e., in absence of wind, increasing snow depths reduce/inhibit surface undulations and promote more spatially continuous snow cover (Filhol and Sturm, 2019). The spatial arrangement of the trees may have a larger control on snow depths in the boreal forest, i.e., forest gaps in the coniferous forest with various slopes and aspects create pronounced and distinct snow depth variabilities inside the forest (Woods et al., 2006). For instance, in Montmorency, superimposed *TWSI* and *LAI* maps (Supplement Fig. S3) show that the high snow depth values associated with *TWSI* values from 10–12 (Fig. 6c) are associated with a forest gap that likely prevents snow interception and accumulates more snow. The counterintuitive preferential snow accumulation on southern slopes in the field at Montmorency could be due to the influence of the various meteorological stations at the site. Our results support the findings of previous studies that the snow depth distribution of the coniferous environments is mainly governed by the canopy characteristics such as structure, distribution, and type of
515 vegetation (Winkler et al., 2005; López-Moreno and Latron, 2008; Varhola et al., 2010a; Zheng et al., 2018; Koutantou et al., 2022). But the microtopography, even under wind-sheltered conditions in the forest, still explains part of the spatial variability.

While not a major focus of our study, we believe our RF model performances, with overall validation R^2 of 0.28–0.52 (Fig. 7), are in an acceptable range for the purpose of our study. All sites have different climates. The higher performance at
520 Sainte-Marthe could be due to a combination of different factors. Early melt of snow due to frequent rain-on-snow events in this region (Paquette and Baraer, 2021) and the presence of basal ice as observed in the field campaign might have contributed to a more structured snowpack in the Sainte-Marthe forest and hence improved the prediction of snow depth compared to the other agro-forested site. Reasonably high R^2 values in agricultural fields at both agro-forested sites (0.39 in Sainte-Marthe and 0.45 in Saint-Maurice) indicate that the models captured the relevant processes through the predictor
525 variables considered. In contrast, Saint-Maurice forest has the worst performance (0.10). This could be due to underlying processes/variables not considered in our model, possibly associated with the canopy structure of the mixed forest. Comparatively low R^2 in Montmorency (0.17) field must have been a result of the concentric snow accumulations patterns around the precipitation gauges and other meteorological instruments that eventually degraded the prediction power of snow depth in the RF model. Moreover, the reduced sampling under coniferous trees due to limited lidar penetration could also
530 have affected grid-scale mean snow depth and resulting relationships with landscape metrics.

The previous studies that used RF model to estimate snow depths/SWE (Bair et al., 2018; Yang et al., 2020) were mainly focused on mountainous watersheds with large elevation gradients and with less or no vegetation and reported average Nash–Sutcliffe efficiencies as high as ~0.7, where the major part of this variance was explained by elevation. In addition, the abundance of studies that employed MLR (Jost et al., 2007; Lehning et al., 2011; Grünwald et al., 2013; Revuelto et al.,
535 2014; Fujihara et al., 2017) and BRT (Winstral et al., 2002; Anderton et al., 2004; Molotch et al., 2005; Revuelto et al., 2014) in alpine environments with rocky outcrops and pasture or no vegetation also reported R^2 of 0.25–0.91 where a substantial portion of the snow depth variability was explained by terrain parameters, mostly elevation. However, model



performances are shown to be degraded with the presence of forests. Studies conducted in forested terrain with relatively small elevation ranges reported R^2 of 0.25–0.51 by MLR (Zheng et al., 2016; Zheng et al., 2018) and BRT (Erxleben et al., 2002; Veatch et al., 2009; Baños et al., 2011). Musselman et al. (2008) proved that including detailed vegetation information like micro-scale vegetation-induced solar radiation, distance to the canopy, and tree bole could improve BRT performance to 0.68 in a forested area. Similarly, our inclusion of small-scale vegetation characteristics and terrain variables in RF model has contributed to an improved model fit (better validation R^2) compared to previous works in forested terrain.

4.4 Limitations of the study

This study provides an insight into the scaling properties of the snowpack and the effect of different topographic, vegetation, and forest edge characteristics on snow depth variability in open versus forested areas with different canopy covers. However, there are potential limitations with some of the methods presented in this study. For instance, despite our efforts to incorporate processes/variables influencing the snow spatial distribution with available data, comparatively lower performance of RF models in Saint-Maurice and Montmorency indicate there could still be some processes/variables we were unable to account for (e.g., soil parameters, snowpack state, and meteorological variables). Especially in Montmorency, there were observation gaps by UAV-lidar due to the thick canopy cover that eventually affected the accuracy of snow depth raster and other variable raster delineations (e.g., slope, LAI, etc.). As well, the aggregation of high-resolution rasters to larger grid sizes for use in the RF models would have averaged some small-scale variations. The dominant predictors might also depend on the timing of the survey date (e.g., near peak snow accumulation versus early and mid-winter, or melt period). Hence, repeat surveys with UAV-lidar to track the temporal evolution of the snowpack would be required to fully address this question in the future.

5 Conclusions

In this study, including wind-related forest edge effects improved the statistical prediction accuracy of snow depth spatial variability by more than 50 % in agro-forested sites, whereas incorporating canopy characteristics improved the predictive accuracy by more than 60 % in the coniferous site. This implies the importance of including and better representing these processes in process-based models. Taken together, our results suggest that in agro-forested landscapes of the St. Lawrence valley, geomorphological assemblages drive the differential snow accumulation between field and forested areas, i.e., rugged glacial deposits with preserved forests favor more snow accumulation whereas flat glaciomarine sediments in the exposed fields promote less snow accumulation and more snow erosion. The blowing snow redistributed from the fields gets trapped in canals/streams and accumulates along the forest edges, accounting for the highest local snow depths in these landscapes. As well, within deciduous/mixed forests, it is rather the underlying topography and/or the forest edges that govern the snow depth variability, while within the coniferous environment, it is the forest structure variability. More often, these processes are not fully represented in process-based models. For instance, most of the process-based models like CRHM (Pomeroy et



570 al., 2007), and SnowModel (Liston and Sturm, 1998) prescribe a single, typical LAI for land cover classes. This ignores the
variability within stands which could compromise larger scale estimates of snowpacks. Our results suggest that snow
redistribution in forest edges, forest structure variability, and better representation of prominent topographical features such
as canals are important processes/variables that should be taken into account in process-based models. This highlights the
advantage of using high resolution data to characterize small-scale processes and therefore explicitly resolve snow depth
variability.

575 In addition, since the selected sites are representative of typical agro-forested and boreal landscapes in southern Québec, the
findings of this study could be applied/extrapolated to similar landscapes in the region and any similar environments where
similar processes operate. It is worth noting that future efforts in designing modeling parameterizations that include forest
edge effects would benefit from incorporating the meteorological conditions together with topographic and vegetation
characteristics.

580

Author Contributions: Conceptualization, C.K.; methodology, C.K. and V.D.; formal analysis, V.D. and C.K.; data
curation, V.D.; writing-original draft preparation, V.D.; writing-review and editing, C.K. and M.B.; supervision, C.K. and
M.B.; project administration, C.K.; funding acquisition, C.K.

585 **Funding:** This study was financially supported by the Canada Research Chair program (grant number 231380) and the
Natural Sciences and Engineering Research Council of Canada (NSERC discovery grant CRSNG-RGPIN-2015-03844)
(Christophe Kinnard) and a doctoral scholarship from the Centre de Recherche sur les Interactions Bassins Versants-
Écosystèmes Aquatiques (RIVE, Vasana Dharmadasa).

Data Availability Statement: The data presented in this study are available on a reasonable request from the corresponding
author.

590 **Acknowledgments:** The authors extend their appreciation to the members of GlacioLab for their help during our fieldwork.
Moreover, the authors are grateful to the Sainte-Marthe municipality, Québec, Canada and members of NEIGE_FM, Forêt
Montmorency, Québec, Canada.

Conflicts of Interest: The authors declare no conflict of interest.

References

- 595 Anderton, S. P., White, S., and Alvera, B.: Evaluation of spatial variability in snow water equivalent for a high mountain
catchment, *Hydrological Processes*, 18, 435–453, doi: 10.1002/hyp.1319, 2004.
- Aygiün, O., Kinnard, C., Campeau, S., and Krogh, S. A.: Shifting hydrological processes in a Canadian agroforested
catchment due to a warmer and wetter climate, *Water*, 12, 739, 2020.
- Bair, E. H., Abreu Calfa, A., Rittger, K., and Dozier, J.: Using machine learning for real-time estimates of snow water
600 equivalent in the watersheds of Afghanistan, *The Cryosphere*, 12, 1579–1594, doi: 10.5194/tc-12-1579-2018, 2018.



- Baños, I. M., García, A. R., Alavedra, J. M. i., Figueras, P. O. i., Iglesias, J. P., Figueras, P. M. i., and López, J. T.: Assessment of airborne lidar for snowpack depth modeling, *Boletín de la Sociedad Geológica Mexicana*, 63(1), 95–107, 2011.
- Blue Marble Geographics: Global Mapper, Blue Marble Geographics, Hallowell, ME, USA, 2020.
- 605 Breiman, L.: Random Forests, *Machine Learning*, 45, 5–32, doi: 10.1023/A:1010933404324, 2001.
- Brown, R. D.: Analysis of snow cover variability and change in Québec, 1948–2005, *Hydrological Processes*, 24, 1929–1954, 2010.
- Broxton, P., Leeuwen, W. J. V., and Biederman, J.: Improving snow water equivalent maps with machine learning of snow survey and lidar measurements, *Water Resour. Res.*, 55, 3739–3757, doi: 10.1029/2018WR024146, 2019.
- 610 Broxton, P. D., Harpold, A. A., Biederman, J. A., Troch, P. A., Molotch, N. P., and Brooks, P. D.: Quantifying the effects of vegetation structure on snow accumulation and ablation in mixed-conifer forests, *Ecohydrology*, 8, 1073–1094, 2015.
- Cho, E., Hunsaker, A. G., Jacobs, J. M., Palace, M., Sullivan, F. B., and Burakowski, E. A.: Maximum entropy modeling to identify physical drivers of shallow snowpack heterogeneity using unpiloted aerial system (UAS) lidar, *Journal of Hydrology*, 602, 126722, doi: 10.1016/j.jhydrol.2021.126722, 2021.
- 615 Currier, W., Pflug, J. M., Mazzotti, G., Jonas, T., Deems, J. S., Bormann, K., Painter, T., Hiemstra, C., Gelvin, A., Uhlmann, Z., Spaete, L., Glenn, N., and Lundquist, J. D.: Comparing aerial lidar observations with terrestrial lidar and snow probe transects from NASA's 2017 SnowEx campaign, *Water Resour. Res.*, 55, 6285–6294, doi: 10.1029/2018WR024533, 2019.
- Currier, W. R. and Lundquist, J. D.: Snow depth variability at the forest edge in multiple climates in the western United States, *Water Resour. Res.*, 54, 8756–8773, doi: 10.1029/2018WR022553, 2018.
- 620 Deems, J. S., Fassnacht, S. R., and Elder, K. J.: Fractal distribution of snow depth from lidar data, *Journal of Hydrometeorology*, 7, 285–297, 2006.
- Deems, J. S., Fassnacht, S. R., and Elder, K. J.: Interannual consistency in fractal snow depth patterns at two Colorado mountain sites, *Journal of Hydrometeorology*, 9, 977–988, doi: 10.1175/2008JHM901.1, 2008.
- Dharmadasa, V., Kinnard, C., and Baraër, M.: An accuracy assessment of snow depth measurements in agro-forested environments by UAV lidar, *Remote Sensing*, 14, 1649, doi: 10.3390/rs14071649, 2022.
- 625 Egli, L., Jonas, T., Grünwald, T., Schirmer, M., and Burlando, P.: Dynamics of snow ablation in a small Alpine catchment observed by repeated terrestrial laser scans, *Hydrological Processes*, 26, 1574–1585, doi: 10.1002/hyp.8244, 2012.
- Elder, K., Michaelsen, J., and Dozier, J.: Small basin modelling of snow water equivalence using binary regression tree methods, *Biogeochemistry of Seasonally Snow-Covered Areas*, IAHS-AIHS and IUGG XXI General Assembly, Boulder, Colorado, July 1995, 129–139, 1995.
- 630 Elder, K., Rosenthal, W., and Davis, R. E.: Estimating the spatial distribution of snow water equivalence in a montane watershed, *Hydrological Processes*, 12, 1793–1808, 1998.
- Environment and Climate Change Canada. Canadian Climate Normals 1981-2010, Edited. Retrieved August 10, 2020 <https://climate.weather.gc.ca/>, 2021a.



- 635 Environment and Climate Change Canada. Hourly Data Report. Retrieved July 16, 2021 <https://climate.weather.gc.ca/>, 2021b.
- Erxleben, J., Elder, K., and Davis, R.: Comparison of spatial interpolation methods for estimating snow distribution in the Colorado Rocky Mountains, *Hydrological Processes*, 16, 3627–3649, 2002.
- Essery, R., Rutter, N., Pomeroy, J., Baxter, R., Stähli, M., Gustafsson, D., Barr, A., Bartlett, P., and Elder, K.: SNOWMIP2
640 an evaluation of forest snow process simulations, *Bulletin of the American Meteorological Society*, 1120–1135, 2009.
- Evans, J. S. and Hudak, A. T.: A multiscale curvature algorithm for classifying discrete return LiDAR in forested environments, *IEEE Transactions on Geoscience and Remote Sensing*, 45, 1029–1038 doi: 10.1109/TGRS.2006.890412, 2007.
- Fassnacht, S. R. and Deems, J. S.: Measurement sampling and scaling for deep montane snow depth data, *Hydrological
645 Processes*, 20, 829–838, 2006.
- Filhol, S. and Sturm, M.: The smoothing of landscapes during snowfall with no wind, *Journal of Glaciology*, 65, 173–187, doi: 10.1017/jog.2018.104, 2019.
- Fujihara, Y., Takase, K., Chono, S., Ichion, E., Ogura, A., and Tanaka, K.: Influence of topography and forest characteristics on snow distributions in a forested catchment, *Journal of Hydrology*, 546, 289–298, 2017.
- 650 Geodetics, I.: Geo-iNAV®, Geo-RelNAV®, Geo-PNT®, Geo-Pointer™, Geo-hNAV™, Geo-MMS™ and Geo-RR™ Commercial User Manual (Document 20134 Rev X), Geodetics, Inc., San Diego, CA, USA, 2018.
- Geodetics, I.: LiDARTool™ User Manual (Document 20149 Rev I), Geodetics, Inc., San Diego, CA, USA, 2019.
- Golding, D. L. and Swanson, R. H.: Snow distribution patterns in clearings and adjacent forest, *Water Resour. Res.*, 22(13), 1931–1940, 1986.
- 655 GreenValley-International: LiDAR360 User Guide, GreenValley International, Ltd, Berkeley, CA, USA, 2020.
- Grünewald, T., Stötter, J., Pomeroy, J., Dadj, R., Baños, I. M., Marturia, J., Spross, M., Hopkinson, C., Burlando, P., and Lehning, M.: Statistical modelling of the snow depth distribution in open alpine terrain, *Hydrology and Earth System Sciences*, 17, 3005–3021, doi: 10.5194/hess-17-3005-2013, 2013.
- Harder, P., Pomeroy, J., and Helgason, W.: Improving sub-canopy snow depth mapping with unmanned aerial vehicles:
660 Lidar versus structure-from-motion techniques, *The Cryosphere*, 14, 1919–1935, doi: 10.5194/tc-14-1919-2020, 2020.
- Harder, P., Schirmer, M., Pomeroy, J., and Helgason, W.: Accuracy of snow depth estimation in mountain and prairie environments by an unmanned aerial vehicle, *The Cryosphere*, 10, 2559–2571, 2016.
- Harpold, A. A., Guo, Q., Molotch, N., Brooks, P. D., Bales, R., Fernandez-Diaz, J. C., Musselman, K. N., and Swetnam, T. L.: Lidar-derived snowpack data sets from mixed conifer forests across the Western United States, *Water Resour. Res.*, 50,
665 2749–2755, 2014.
- Hedstrom, N. R. and Pomeroy, J. W.: Measurements and modelling of snow interception in the boreal forest, *Hydrological Processes*, 12, 1611–1625, 1998.



- Hojatimalekshah, A., Uhlmann, Z., Glenn, N., Hiemstra, C., Tennant, C., Graham, J., Spaete, L., Gelvin, A., Marshall, H., McNamara, J., and Enterkine, J.: Tree canopy and snow depth relationships at fine scales with terrestrial laser scanning, *The Cryosphere*, 15, 2187–2209, doi: 10.5194/tc-15-2187-2021, 2021.
- Hopkinson, C., Sitar, M., Chasmer, L., and Treitz, P.: Mapping snowpack depth beneath forest canopies using airborne lidar, *Photogrammetric Engineering & Remote Sensing*, 70, 323–330, 2004.
- Hopkinson, C., Collins, T., Anderson, A., Pomeroy, J., and Spooner, I.: Spatial snow depth assessment using lidar transect samples and public GIS data layers in the Elbow River watershed, Alberta, Canadian Water Resources Journal, 37, 69–87, 2012.
- Hopkinson, C., Pomeroy, J., Debeer, C., Ellis, C., and Anderson, A.: Relationships between snowpack depth and primary lidar point cloud derivatives in a mountainous environment, *Remote Sensing and Hydrology*, Jackson Hole, Wyoming, USA, 27–30 September 2010, 2012.
- Jacobs, J. M., Hunsaker, A. G., Sullivan, F. B., Palace, M., Burakowski, E. A., Herrick, C., and Cho, E.: Snow depth mapping with unpiloted aerial system lidar observations: a case study in Durham, New Hampshire, United States, *The Cryosphere*, 15, 1485–1500, doi: 10.5194/tc-15-1485-2021, 2021.
- Jost, G., Weiler, M., Gluns, D. R., and Alila, Y.: The influence of forest and topography on snow accumulation and melt at the watershed-scale, *Journal of Hydrology*, 347, 101–115, 2007.
- Kirchner, P. B., Bales, R. C., Molotch, N. P., Flanagan, J., and Guo, Q.: Lidar measurement of seasonal snow accumulation along an elevation gradient in the southern Sierra Nevada, California, *Hydrology and Earth System Sciences*, 18, 4261–4275, 2014.
- Koutantou, K., Mazzotti, G., and Brunner, P.: UAV-based lidar high-resolution snow depth mapping in the swiss alps: Comparing flat and steep forests, *Int. Arch. Photogramm. Remote Sens. Spatial Inf. Sci.*, XLIII-B3-2021, 477–484, doi: 10.5194/isprs-archives-XLIII-B3-2021-477-2021, 2021.
- Koutantou, K., Mazzotti, G., Brunner, P., Webster, C., and Jonas, T.: Exploring snow distribution dynamics in steep forested slopes with UAV-borne LiDAR, *Cold Regions Science and Technology*, 200, 103587, doi: 10.1016/j.coldregions.2022.103587, 2022.
- Lehning, M., Grünewald, T., and Schirmer, M.: Mountain snow distribution governed by an altitudinal gradient and terrain roughness, *Geophysical Research Letters*, 38, L19504, doi: 10.1029/2011GL048927, 2011.
- Lendzioch, T., Langhammer, J., and Jenicek, M.: Tracking forest and open area effects on snow accumulation by unmanned aerial vehicle photogrammetry, *International Archives of the Photogrammetry, Remote Sensing and Spatial Information Sciences*, XLI-B1, 917–923, 2016.
- Li, W., Guo, Q., Jakubowski, M. K., and Kelly, M.: A new method for segmenting individual trees from the lidar point cloud, *Photogrammetric Engineering & Remote Sensing*, 78(1), 75–84, 2012.
- Liston, G. E. and Elder, K.: A distributed snow-evolution modeling system (SnowModel), *Journal of Hydrometeorology*, 7, 1259–1276, 2006.



- Liston, G. E. and Sturm, M.: A snow-transport model for complex terrain, *Journal of Glaciology*, 44(148), 498–516, 1998.
- López-Moreno, J. I. and Latron, J.: Spatial heterogeneity in snow water equivalent induced by forest canopy in a mixed beech-fir stand in the Pyrenees, *Annals of Glaciology*, 49, 83–90, 2008.
- 705 Mazzotti, G., Currier, W., Deems, J. S., Pflug, J. M., Lundquist, J. D., and Jonas, T.: Revisiting snow cover variability and canopy structure within forest stands: Insights from airborne lidar data, *Water Resour. Res.*, 55, 6198–6216, doi: 10.1029/2019WR024898, 2019.
- Mendoza, P. A., Musselman, K. N., Revuelto, J., Deems, J. S., López-Moreno, J. I., and McPhee, J.: Interannual and seasonal variability of snow depth scaling behavior in a subalpine catchment, *Water Resour. Res.*, 56, e2020WR027343, doi: 710 10.1029/2020WR027343, 2020.
- Molotch, N. P., Colee, M. T., Bales, R. C., and Dozier, J.: Estimating the spatial distribution of snow water equivalent in an alpine basin using binary regression tree models: The impact of digital elevation data and independent variable selection, *Hydrological Processes*, 19, 1459–1479, 2005.
- Morsdorf, F., Kötz, B., Meier, E., Itten, K. I., and Allgöwer, B.: Estimation of LAI and fractional cover from small footprint 715 airborne laser scanning data based on gap fraction, *Remote Sensing of Environment*, 104, 50–61, 2006.
- Mott, R., Schirmer, M., and Lehning, M.: Scaling properties of wind and snow depth distribution in an Alpine catchment, *Journal of Geophysical Research*, 116, D06106, doi: 10.1029/2010JD014886, 2011.
- Musselman, K. N., Molotch, N. P., and Brooks, P. D.: Effects of vegetation on snow accumulation and ablation in a mid-latitude sub-alpine forest, *Hydrological Processes*, 22, 2767–2776, doi: 10.1002/hyp.7050, 2008.
- 720 Painter, T., Berisford, D., Boardman, J., Bormann, K. J., Deems, J., Gehrke, F., Hedrick, A., Joyce, M., Laidlaw, R., Marks, D., Mattmann, C., Mcgurk, B., Ramirez, P., Richardson, M., Skiles, S., Seidel, F., and Winstral, A.: The Airborne Snow Observatory: Fusion of scanning lidar, imaging spectrometer, and physically-based modeling for mapping snow water equivalent and snow albedo, *Remote Sensing of Environment*, 184, 139–152, 2016.
- Paquette, A. and Baraer, M.: Hydrological behavior of an ice-layered snowpack in a non-mountainous environment, 725 *Hydrological Processes*, 36, e14433, doi: 10.1002/hyp.14433, 2021.
- Plattner, C., L. N. , A., B., and Brenning: The spatial variability of snow accumulation on Vernagtferner, Austrian Alps, in Winter 2003/2004, *Zeitschrift für Gletscherkunde und Glazialgeologie*, 39, 43–57, 2004.
- Pomeroy, J. W. and Granger, R. J.: Sustainability of the western Canadian boreal forest under changing hydrological conditions-Snow accumulation and ablation, *Sustainability of Water Resources under Increasing Uncertainty (Proceedings of an international Symposium S1)*, Rabat, Morocco, 23 April–3 May 1997, 237–242, 1997.
- 730 Pomeroy, J. W., Parviainen, J., Hedstrom, N., and Gray, D. M.: Coupled modelling of forest snow interception and sublimation, *Hydrological Processes*, 12, 2317–2337, 1998.
- Pomeroy, J. W., Gray, D. M., Brown, T., Hedstrom, N. R., Quinton, W. L., Granger, R. J., and Carey, S. K.: The cold regions hydrological model: a platform for basing process representation and model structure on physical evidence, 735 *Hydrological Processes*, 21, 2650–2667, doi: 10.1002/hyp.6787, 2007.



- Proulx, H., Jacobs, J. M., Burakowski, E. A., Cho, E., Hunsaker, A. G., Sullivan, F. B., Palace, M., and Wagner, C.: Comparison of in-situ snow depth measurements and impacts on validation of unpiloted aerial system lidar over a mixed-use temperate forest landscape, *The Cryosphere Discuss.* [preprint], doi: 10.5194/tc-2022-7, in review, 2022.
- 740 Revuelto, J., López-Moreno, J., Azorin-Molina, C., and Vicente-Serrano, S. M.: Topographic control of snowpack distribution in a small catchment in the central Spanish Pyrenees: Intra- and inter-annual persistence, *The Cryosphere*, 8, 1989–2006, doi: 10.5194/tc-8-1989-2014, 2014.
- Richardson, J. J., Moskal, L. M., and Kim, S.-H.: Modeling approaches to estimate effective leaf area index from aerial discrete-return lidar, *Agricultural and Forest Meteorology*, 149, 1152–1160, 2009.
- Roth, T. R. and Nolin, A. W.: Forest impacts on snow accumulation and ablation across an elevation gradient in a temperate
745 montane environment, *Hydrology and Earth System Sciences*, 21, 5427–5442, 2017.
- Royer, A., Roy, A., Jutras, S., and Langlois, A.: Review article: Performance assessment of radiation-based field sensors for monitoring the water equivalent of snow cover (SWE), *The Cryosphere*, 15, 5079–5098, doi: 10.5194/tc-15-5079-2021, 2021.
- Schirmer, M. and Lehning, M.: Persistence in intra-annual snow depth distribution: 2. Fractal analysis of snow depth
750 development, *Water Resour. Res.*, 47, W09517, doi: 10.1029/2010WR009429, 2011.
- Sena, N., Chokmani, K., Gloaguen, E., and Bernier, M.: Analyse multi-échelles de la variabilité spatiale de l'équivalent en eau de la neige (EEN) sur le territoire de l'Est du Canada, *Hydrological Sciences Journal*, 62(3), 359–377, 2017.
- SPH-Engineering: UgCS Desktop application version 3.2 (113) User Manual, SPH Engineering, Baložu Pilsēta, Latvia, 2019.
- 755 Tinkham, W. T., Smith, A. M. S., Marshall, H., Link, T., Falkowski, M., and Winstral, A.: Quantifying spatial distribution of snow depth errors from lidar using random forest, *Remote Sensing of Environment*, 141, 105–115, doi: 10.1016/j.rse.2013.10.021, 2014.
- Trujillo, E., Ramí' rez, J. A., and Elder, K. J.: Topographic, meteorologic, and canopy controls on the scaling characteristics of the spatial distribution of snow depth fields, *Water Resour. Res.*, 43, W07409, 1–17, 2007.
- 760 Trujillo, E., Ramírez, J. A., and Elder, K.: Scaling properties and spatial organization of snow depth fields in sub alpine forest and alpine tundra, *Hydrological Processes*, 23, 1575–1590, doi: 10.1002/hyp.7270, 2009.
- Tyralis, H., Papacharalampous, G., and Langousis, A.: A brief review of random forests for water scientists and practitioners and their recent history in water resources, *Water*, 11, 910, 2019.
- Valence, E., Baraer, M., Rosa, E., Barbecot, F., and Monty, C.: Introducing drone-based GPR in snow hydrology studies,
765 *The Cryosphere Discuss.* [preprint], doi: 10.5194/tc-2022-42, in review, 2022.
- Varhola, A., Coops, N. C., Weiler, M., and Moore, R. D.: Forest canopy effects on snow accumulation and ablation: An integrative review of empirical results, *Journal of Hydrology*, 392, 219–233, 2010a.



- 770 Varhola, A. s., Coops, N. C., Bater, C. W., Teti, P., Boon, S., and Weiler, M.: The influence of ground- and lidar-derived forest structure metrics on snow accumulation and ablation in disturbed forests, *Canadian Journal of Forest Research*, 40, 812–821, 2010b.
- Veatch, W., Brooks, P. D., Gustafson, J. R., and Molotch, N. P.: Quantifying the effects of forest canopy cover on net snow accumulation at a continental, mid-latitude site, *Ecohydrology*, 2, 115–128, 2009.
- Webster, R. and Oliver, M.: *Geostatistics for environmental scientists*, second edition, in, Chichester, England: John Wiley & Sons Ltd., doi: 10.1002/9780470517277.ch1, 2007.
- 775 Winkler, R. D., Spittlehouse, D. L., and Golding, D. L.: Measured differences in snow accumulation and melt among clearcut, juvenile, and mature forests in southern British Columbia, *Hydrological Processes*, 19, 51–62, 2005.
- Winstral, A. and Marks, D.: Simulating wind fields and snow redistribution using terrain based parameters to model snow accumulation and melt over a semi arid mountain catchment, *Hydrological Processes*, 16, 3585–3603, doi: 10.1002/hyp.1238, 2002.
- 780 Winstral, A., Elder, K., and Davis, R. E.: Spatial snow modeling of wind-redistributed snow using terrain-based parameters, *Journal of Hydrometeorology*, 3, 524–538, doi: 10.1175/1525-7541(2002)003<0524:Ssmowr>2.0.Co;2, 2002.
- Woods, S. W., Ahl, R., Sappington, J., and McCaughey, W.: Snow accumulation in thinned lodgepole pine stands, Montana, USA, *Forest Ecology and Management*, 235, 202–211, 2006.
- Yang, J., Jiang, L., Luo, K., Pan, J., Lemmetyinen, J., Takala, M., and Wu, S.: Snow depth estimation and historical data reconstruction over China based on a random forest machine learning approach, *The Cryosphere*, 14, 1763–1778, doi: 10.5194/tc-14-1763-2020, 2020.
- 785 Zhang, X., Gao, R., Sun, Q., and Cheng, J.: An automated rectification method for unmanned aerial vehicle LiDAR point cloud data based on laser intensity, *Remote Sensing*, 11, 811, doi: 10.3390/rs11070811, 2019.
- Zheng, Z., Kirchner, P. B., and Bales, R. C.: Topographic and vegetation effects on snow accumulation in the southern Sierra Nevada: A statistical summary from lidar data, *The Cryosphere*, 10, 257–269, 2016.
- 790 Zheng, Z., Ma, Q., Qian, K., and Bales, R. C.: Canopy effects on snow accumulation: observations from lidar, canonical-view photos, and continuous ground measurements from sensor networks, *Remote Sensing*, 10, 1769, doi: 10.3390/rs10111769, 2018.
- Zheng, Z., Ma, Q., Jin, S., Su, Y., Guo, Q., and Bales, R. C.: Canopy and terrain interactions affecting snowpack spatial patterns in the Sierra Nevada of California, *Water Resour. Res.*, 55, 8721–8739, doi: 10.1029/2018wr023758, 2019.
- 795